Design, Modeling, and Numerical Characteristics of the Plasmonic Dipole Nano-Antennas for Maximum Field Enhancement

Thi Thanh Kieu Nguyen [1], Quang Minh Ngo [2], and Truong Khang Nguyen [3,4,*]

[1] Faculty of Engineering, Binh Thuan Province Vocational College, Binh Thuan, Vietnam

[2] Institute of Materials Science, Vietnam Academy of Science and Technology
18 Hoang Quoc Viet, Cau Giay, Hanoi, Vietnam

[3] Division of Computational Physics, Institute for Computational Science
Ton Duc Thang University, Ho Chi Minh City, Vietnam

[4] Faculty of Electrical and Electronics Engineering, Ton Duc Thang University, Ho Chi Minh City, Vietnam
*nguyentruongkhang@tdt.edu.vn

Abstract **─** In this paper, we investigate the near-field enhanced optical absorption and far-field radiation characteristics of plasmonic dipole nano-antenna with different geometries which are rectangular, square, circular, and ellipse dipoles. Localized E-field enhancement at the excitation gap and reflection profile in an infinite 2D array of each nano-antenna are characterized and optimized at the resonant frequency of 375 THz, which corresponds to the incident wavelength of 800 nm. Numerical results show that the ellipse nano-antenna produces the most enhanced electric field at the excitation gap whereas the circular nano-antenna yields the best reflection and far-field radiation characteristics. This research is useful for the researchers and designers in choosing appropriate plasmonic dipole nano-antennas when incorporating with a photoconductive antenna for terahertz radiation enhancement.

Index Terms **─** Absorption, far-field power pattern, localized electric field, nano-antenna, reflection, surface plasmon resonance.

I. INTRODUCTION

The interaction of light with plasmonic nano-structures has constituted a central research topic in current science and engineering and has been finding several interesting applications in nanophotonic technology [1–4]. Two main demands for existing and emerging nano-optical applications are an optical spot beyond the diffraction limit and a high transparent efficiency. Plasmonic nano-antennas can concentrate the excitation light beam based on the localized surface plasmon resonance and thus can be used in the nano-optical system because of their ability to obtain a very small optical spot. In addition, the enhanced intensity of light confinement into a high index substrate can be achieved by asymmetric scattering due to surface plasmon excited on metallic nanostructures. Consequently, plasmonic nano-antenna can provide high transmission efficiency for practical applications. Recent reports on applications of plasmonic nano-antennas include sensitive photodetection [5], plasmon-emitting diode [6, 7], photovoltaic devices [8], surface enhanced Raman spectroscopy [9], bio-sensing [10], terahertz photoconductive antenna [11–13], etc.

To maximize the field enhancement in the high field region of the optical nano-antenna, which is well-known as the most important parameter to characterize the performance of the nano-antenna, parameters such as antenna geometry, dielectric loading, as well as the polarization of incident light have to be carefully optimized and fined-tune [14, 15]. The optical properties of different types of nano-antennas for the enhancement of fluorescence of molecules have been discussed and demonstrated over the last decades [16–21]. However, a detailed comparison of nano-antennas having different geometries in term of near-field optical absorption and far-field radiation characteristics is still lack in the literature. Therefore, the aim of this paper is to provide such a detailed study and comparison. Four plasmonic dipole nano-antennas with different geometries are chosen for the study and comparison; they are rectangular dipole, square dipole, circular dipole, and ellipse dipole. Absorption and reflection profiles of each nano-antenna are characterized and optimized at the resonant frequency of 375 THz which corresponds to the incident wavelength of 800 nm. The paper is organized as follows: Section 2 presents the nano-antenna geometries and simulation approach; Section 3 presents the results and discussion; Section 4 gives a

Submitted On: July 15, 2016
Accepted On: April 8, 2017

conclusion.

II. GEOMETRY AND MODELLING OF THE NANO-ANTENNAS

Figure 1 shows the geometry of the four nano-antennas under examination in the side and top views. Both the four dipoles and the ground are made of gold. The dipole nano-antenna and the ground are separated by a SiO_2 substrate which having a thickness of T. The widths and the lengths of the rectangular dipole are designated as W_R and L_R, while those of the square dipole are W_S and L_S, those of the circular dipole are W_C and L_C, and those of the ellipse dipole are W_E and L_E, respectively. The SiO_2 thicknesses of each nano-antenna are denoted as T_R, T_S, T_C, T_E whereas the periodicities of each nano-antenna in their arrays are denoted as P_R, P_S, P_C, P_E for the rectangular, square, circular, and ellipse dipoles, respectively. The excitation gap and the gold metal thickness of each nano-antenna are g and T_{Au} = 25 nm, respectively. Design parameters of the four antennas for the optimized localized E-field and reflection coefficient at the desired frequency of 375 THz are as follows: for the rectangular dipole (g = 10 nm, W_R = 35 nm, L_R = 174 nm, T_R = 100 nm, P_R = 550 nm); for the square dipole (g = 10 nm, W_S = 78 nm, L_S = 166 nm, T_S = 40 nm, P_S = 600 nm); for the circular dipole (g = 10 nm, W_C = 94 nm, L_C = 198 nm, T_C = 60 nm, P_C = 590 nm); for the ellipse dipole (g = 10 nm, W_E = 40 nm, L_E = 190 nm, T_E = 70 nm, P_E = 570 nm).

In this paper, a full-wave electromagnetic simulator Microwave Studio by CST based on Finite Integration Technique (FIT) was used to analyze the characteristics of the nano-antennas [22]. Figure 2 (a) shows the model to study the localized E-field response at the excitation gap of the dipoles in which the excitation source is a plane wave incident from the top with an electric field amplitude of 1 V/m and with a polarization along the main axis, i.e., x-axis, of the nano-antennas. To detect the localized E-field, a probe was placed in the gap between the dipole arms and oriented along the x-axis. This simulation model also allows calculating the far-field power patterns of the nano-antennas. The transmission/reflection coefficient of the nano-antenna was studied by using a unit cell model that employed a two-Floquet-port model with electric and magnetic boundary conditions enforced along the $\pm x$ and $\pm y$ directions, seen in Fig. 2 (b). The Au metal and SiO_2 substrates used in the simulation can be defined in the material library of the CST MWS software. Figure 3 shows the electric dispersion curves of Au and SiO_2 within the frequency range of interest, i.e., 200 THz - 500 THz which these close to the measured values in the previously reported studies [23, 24].

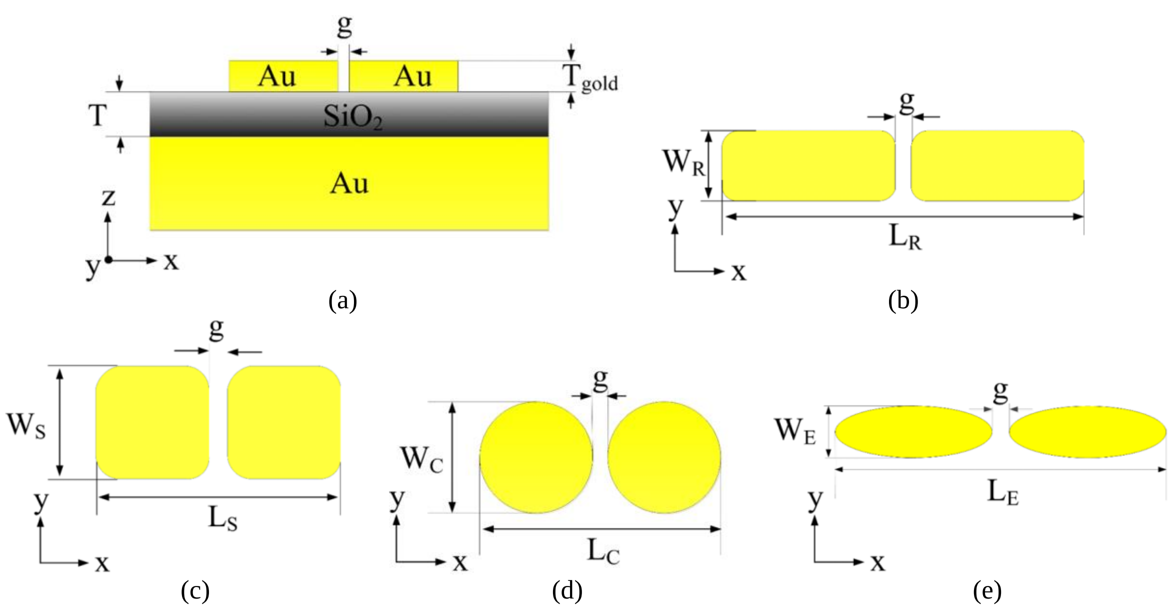

Fig. 1. (a) Side view of the nano-antennas; (b-e) geometries of the rectangular dipole, square dipole, circular dipole, and ellipse dipole.

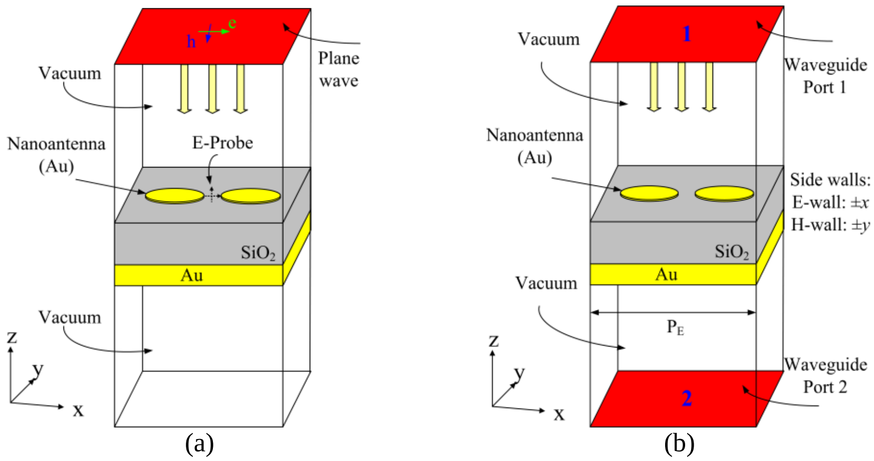

Fig. 2. Simulation models: (a) to calculate the localized E-field and far-field power pattern, and (b) to calculate the reflection coefficient of an infinite 2D array.

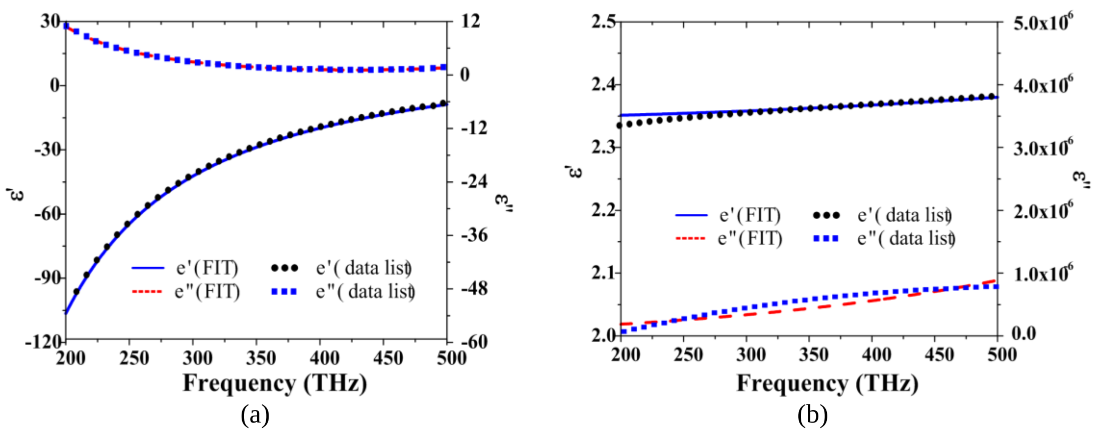

Fig. 3. Dispersion curves of: (a) gold and (b) SiO_2 in the frequency of interest from 200 THz to 500 THz.

III. RESULTS AND DISCUSSION

We select the ellipse dipole nano-antenna to investigate the frequency response on the design parameters (g, T_E, L_E, and P_E) since other three nano-antennas was observed to behave identically. It is noted that in this parameter study, one parameter was varied whereas others were fixed. In addition, hereinafter F_{peak} denotes the frequency where occurring the maximum localized electric field E_{peak}. Figure 4 (a) shows that the excitation gap, g, strongly influences the electric field confinement. The narrower the g is, the lower the resonant frequency occurred, and the significantly better the localized E_{peak} presented. Maximum E_{peak} could reach to approximately 400 V/m when g decreases to 7 nm. For the optimized design, we chose g = 10 nm because of the two reasons: first, if g = 10 nm, the resonant frequency occurring the maximum E_{peak} was mostly close to the desired frequency of 375 THz; second, if g is so small, we would encounter a short circuit problem after the fabrication process. Figure 4 (b) shows that when the thickness of the SiO_2 layer T_E changed, both F_{peak} and E_{peak} significantly changed, and clearly demonstrated a resonance behavior. When T_E increased from 20 nm to 100 nm with a step of 20 nm, F_{peak} increased, reached a maximum value, and then decreased and similarly for E_{peak}. At T_E = 70 nm, F_{peak} was mostly close to the desired frequency of 375 THz, and E_{peak} reached the maximum value. This behavior is interesting, which was proven in [14] and said that the distance from the nano-antenna to the reflective surface (Au ground) must be selected to satisfy the resonance condition if we consider the SiO_2 substrate layer as an Fabry-Perot resonator cavity.

Figure 4 (c) shows that when L_E increased, F_{peak} decreased, which follows the theory that the antenna length is inversely proportional to its operating frequency. We can calculate the effective wavelength according to the formula as:

$$\lambda_{eff} = \frac{\lambda_0}{\sqrt{\varepsilon_{eff}}} = \frac{c}{f_0\sqrt{\varepsilon_{eff}}}, \qquad (1)$$

where c is the speed of light (3×10^8 m/s), f_o is the resonant frequency (~ 375 THz), and ε_{eff} the effective dielectric constant of SiO_2 (~ 2.4). Accordingly, the effective wavelength is approximately 510 nm. In theory, the antenna has a length of about a half of the effective wavelength (L_{total} ~ $\lambda_{eff}/2$ ~ 260 nm) will present the first resonance mode. The resulted nano-antenna length in our simulation is approximately of 200 nm which is shorter than the theoretically predicted length. This can be attributed to an increase of the effective permittivity of the whole structure due to the presence of the reflecting mirror Au. When we consider the localized E-field, the total length of the nano-antennas also influenced the E_{peak}. The value of L_E = 190 nm exhibited the maximum E_{peak} of 150 V/m at the F_{peak} of 374 THz. Figure 4 (d) shows that if the width P_E of the SiO_2 layer, i.e., the periodicity in a 2D infinite array, increased, the resonant frequency decreased, however E_{peak} at the gap increased. The increased width of the semiconductor layer resulted in an increase of the effective permittivity of the whole structure. For the desired resonant frequency around the 375 THz, P_E was chosen to be 570 nm. It can be seen that this parameter is the least influence factor on either E_{peak} or F_{peak}. By investigating the design parameter study of the ellipse geometry, we can conclude that the excitation gap area significantly influenced the localized E-field, while the dipole length decided the resonant frequency of the nano-antennas. More importantly, the thickness of the semiconductor layer must be appropriately chosen to obtain the additional E-field enhancement thanks to the mechanism similar to a Fabry-Perot resonant cavity. These characteristics are identical for the rectangular, square, and circular dipoles.

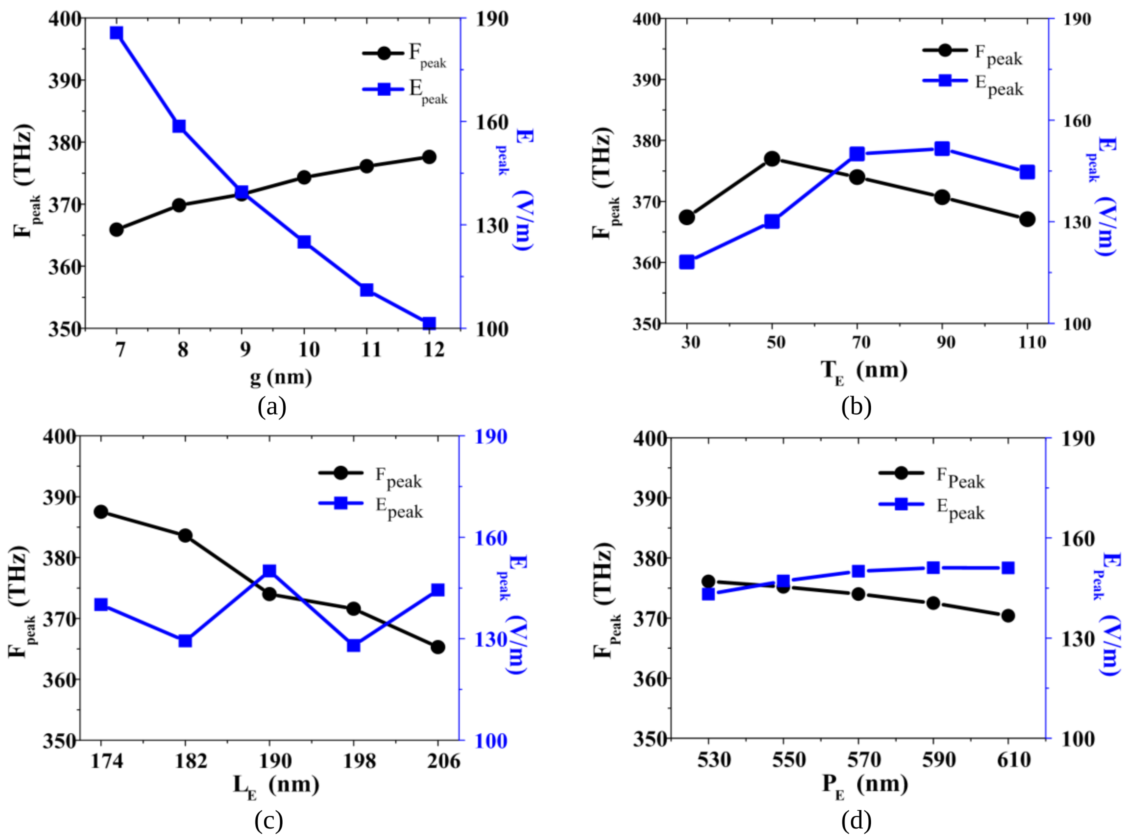

Fig. 4. Parameter study in terms of F_{peak} and E_{peak} of the ellipse dipole: (a) gap between dipole arms, (b) SiO_2 thickness, (c) total dipole length, and (d) lateral size of the SiO_2 substrate.

Figure 5 shows the localized E-field checked at the excitation gap, and the reflection coefficient checked for a 2D infinite array of the four nano-antennas. The optimized results show that the localized E-field of the rectangular dipole was 110.3 V/m at 374.9 THz, while that of the square dipole was 92.2 V/m at 372.8 THz, that of the circular dipole was 125 V/m at 374.3 THz, and that of the ellipse dipole was 150 V/m at 374 THz, seen in Fig. 5 (a). It should be noted that the incident E-field was chosen of 1 V/m. All the four nano-antennas produced a significantly enhanced localized E-field at the gap between the dipole arms. The ellipse dipole produced the highest localized E-field while the square dipole presented the lowest value. In the perspective of the reflection coefficient, the behavior was different. The reflection coefficient of the rectangular dipole was about 0.19 whereas that of the square dipole, circular dipole and ellipse dipole were about 0.28, 0.11, and 0.25, respectively, seen in Fig. 5 (b) (refer to Table 1). Therefore, the circular dipole produced the best reflection characteristic while the square dipole presented the worst case. It is obvious that the resonant frequency F_{peak}, the frequency occurring E_{peak}, almost coincided with the frequency occurring the minimum reflection coefficient. This indicates that the four nano-antenna structures operate well at the desired frequency of 375 THz and thereby maximizing the incident light absorption efficiency.

Figures 6 and 7 respectively present the near-field distribution and the far-field power patterns of the four nano-antennas at their resonant frequencies. The field was mostly distributed in the excitation gaps and at the dipole ends as in a conventional RF dipole. It is obvious that the circular dipole exhibited the best power patterns with the least back radiation in comparison with the three remains. Generally, the ellipse dipole nano-antenna produces the best localized E-field enhancement at the excitation gap whereas the circular dipole nano-antenna yields the best reflection and far-field radiation characteristics. In other words, the circular nano-antenna should be chosen regarding the far-field radiated power while the ellipse nano-antenna should be chosen for the demand of highly localized E-field.

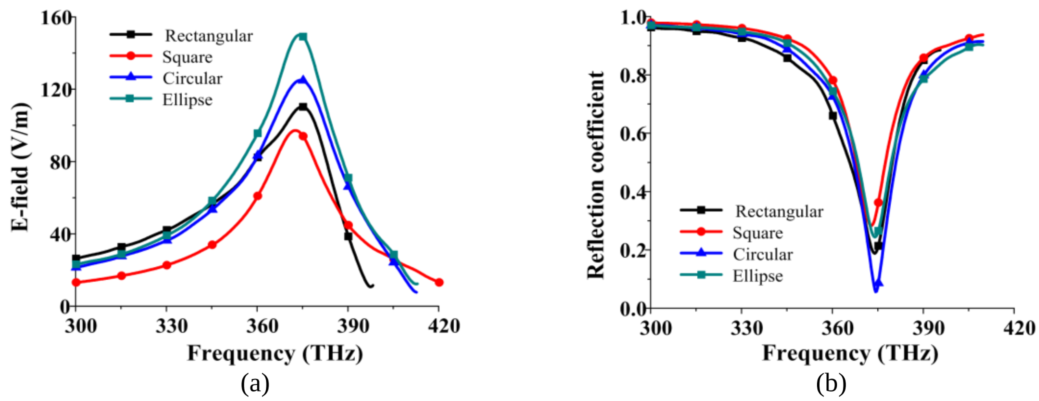

Fig. 5. (a) Localized E-field and (b) reflection coefficient as a function of frequency of the four nano-antennas.

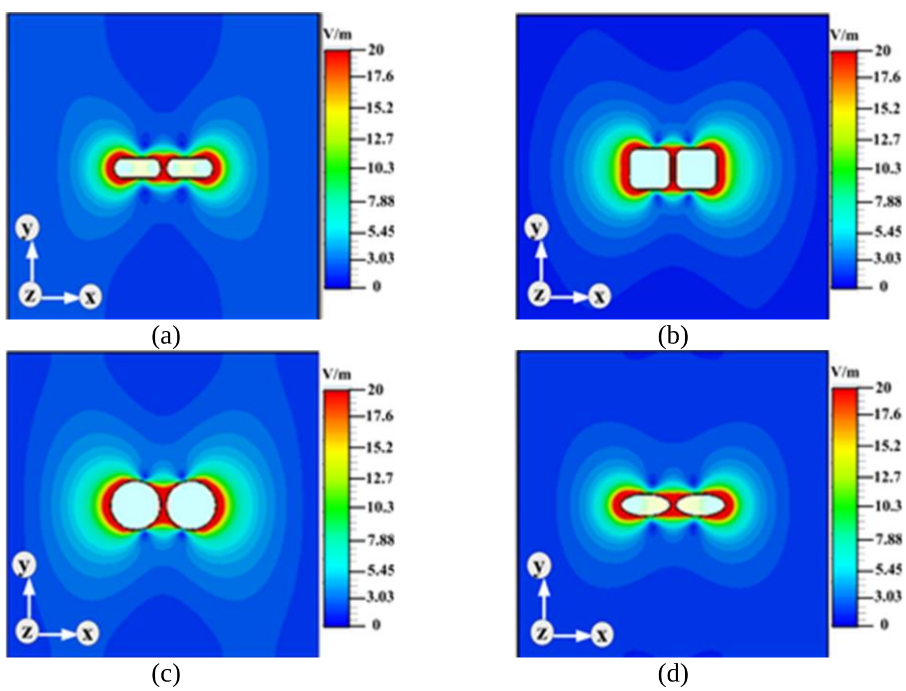

Fig. 6. Field distributions checked at the resonant frequencies of the four nano-antennas: (a) rectangular, (b) square, (c) circular, and (d) ellipse dipoles. The resonant frequencies for each nano-antenna can be refered in Table 1.

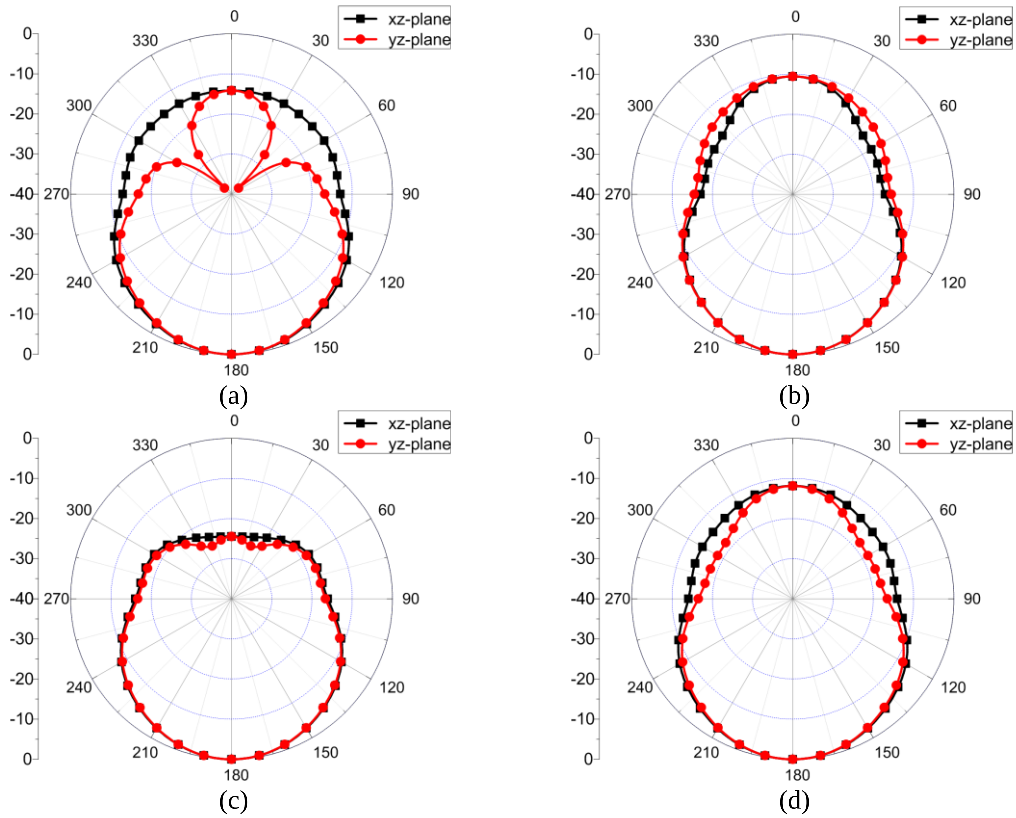

Fig. 7. Normalized far-field E-patterns calculated at the resonant frequencies of the four nano-antennas: (a) rectangular, (b) square, (c) circular, (d) ellipse dipoles. The resonant frequency for each nano-antenna can be referred in Table 1.

Table 1: Optimized results of the four nano-antennas

Geometry	Resonant Frequency F_{peak} (THz)	Localized E-field E_{peak} (V/m)	Reflection Coefficient
Rectangular	374.9	110.3	0.19
Square	372.8	92.2	0.28
Circular	374.3	125.0	0.11
Ellipse	374	150	0.25

IV. CONCLUSION

We have investigated and compared the performance of plasmonic nano-antennas for different geometries such as rectangular, square, circular, and ellipse dipoles. The excitation gap area significantly influenced the localized E-field enhancement, while the dipole length decided the resonant frequency of the nano-antennas. More importantly, the thickness of the semiconductor layers must be appropriately chosen to obtain the additional E-field enhancement thanks to the mechanism similar to a Fabry-Perot resonant cavity. The optimized results show that the ellipse dipole exhibits its outstanding performance regarding the localized E-field enhancement, whereas the circular dipole yields its outstanding performance in terms of the reflection coefficient and the far-field power pattern. This study could be useful for the incorporation of an array of such plasmonic nano-antennas at the active area of photomixer/photoconductive antenna for an efficiency improvement.

ACKNOWLEDGMENT

T. K. Nguyen would like to thank TWAS (16-184 RG/PHYS/AS_I-FR3240293349) for equipment support.

REFERENCES

[1] C. Zhou, Y. Fainman, and Y. Sheng, “Applications of nano-optics,” *Appl. Opt.*, vol. 50, no. 31, pp. N1-NO1, 2011.

[2] J. Wei, *Nonlinear Super-Resolution Nano-Optics and Applications*. Springer, 2015.

[3] A. Fratalocchi, C. M. Dodson, R. Zia, P. Genevet, E. Verhagen, H. Altug, and V. J. Sorger, “Nano-optics gets practical,” *Nat. Nanotechnol.*, vol. 10, no. 1, pp. 11-15, 2015.

[4] J. Chao, Y. Lin, H. Liu, L. Wang, and C. Fan,

"DNA-based plasmonic nanostructures," *Mater. Today*, vol. 18, no. 6, pp. 326-335, 2015.
[5] C. Chakraborty, R. Beams, K. M. Goodfellow, G. W. Wicks, L. Novotny, and A. N. Vamivakas, "Optical antenna enhanced graphene photo-detector," *Appl. Phys. Lett.*, vol. 105, no. 24, p. 241114, 2014.
[6] D. M. Koller, A. Hohenau, H. Ditlbacher, N. Galler, F. Reil, F. R. Aussenegg, A. Leitner, E. J. W. List, and J. R. Krenn, "Organic plasmon-emitting diode," *Nat. Photonics*, vol. 2, no. 11, pp. 684-687, 2008.
[7] M. S. Eggleston, K. Messer, L. Zhang, E. Yablonovitch, and M. C. Wu, "Optical antenna enhanced spontaneous emission," *Proc. Natl. Acad. Sci.*, vol. 112, no. 6, pp. 1704-1709, 2015.
[8] S.-K. Kim, X. Zhang, D. J. Hill, K.-D. Song, J.-S. Park, H.-G. Park, and J. F. Cahoon, "Doubling absorption in nanowire solar cells with dielectric shell optical antennas," *Nano Lett.*, vol. 15, no. 1, pp. 753-758, 2014.
[9] I. Maouli, A. Taguchi, Y. Saito, S. Kawata, and P. Verma, "Optical antennas for tunable enhancement in tip-enhanced Raman spectroscopy imaging," *Appl. Phys. Express*, vol. 8, no. 3, p. 32401, 2015.
[10] A. Singh, J. T. Hugall, G. Calbris, and N. F. van Hulst, "Fiber-based optical nanoantennas for single-molecule imaging and sensing," *J. Light. Technol.*, vol. 33, no. 12, pp. 2371-2377, 2015.
[11] S.-G. Park, K. H. Jin, M. Yi, J. C. Ye, J. Ahn, and K.-H. Jeong, "Enhancement of terahertz pulse emission by optical nanoantenna," *ACS Nano*, vol. 6, no. 3, pp. 2026-2031, 2012.
[12] M. Jarrahi, "Advanced photoconductive terahertz optoelectronics based on nano-antennas and nano-plasmonic light concentrators," *Terahertz Sci. Technol. IEEE Trans.*, vol. 5, no. 3, pp. 391-397, 2015.
[13] A. Jooshesh, V. Bahrami-Yekta, J. Zhang, T. Tiedje, T. E. Darcie, and R. Gordon, "Plasmon-enhanced below bandgap photoconductive terahertz generation and detection," *Nano Lett.*, vol. 15, no. 12, pp. 8306-8310, 2015.
[14] H. Fischer and O. J. F. Martin, "Engineering the optical response of plasmonic nanoantennas," *Opt. Express*, vol. 16, no. 12, pp. 9144-9154, 2008.
[15] T. J. Seok, A. Jamshidi, M. Kim, S. Dhuey, A. Lakhani, H. Choo, P. J. Schuck, S. Cabrini, A. M. Schwartzberg, and J. Bokor, "Radiation engineering of optical antennas for maximum field enhancement," *Nano Lett.*, vol. 11, no. 7, pp. 2606-2610, 2011.
[16] F. J. González and G. D. Boreman, "Comparison of dipole, bowtie, spiral and log-periodic IR antennas," *Infrared Phys. Technol.*, vol. 46, no. 5, pp. 418-428, 2005.
[17] E. G. Mironov, Z. Li, H. T. Hattori, K. Vora, H. H. Tan, and C. Jagadish, "Titanium nano-antenna for high-power pulsed operation," *Light. Technol. J.*, vol. 31, no. 15, pp. 2459-2466, 2013.
[18] I. S. Maksymov, I. Staude, A. E. Miroshnichenko, and Y. S. Kivshar, "Optical Yagi-Uda nanoantennas," *Nanophotonics*, vol. 1, no. 1, pp. 65-81, 2012.
[19] E. G. Mironov, A. Khaleque, L. Liu, I. S. Maksymov, and H. T. Hattori, "Enhancing weak optical signals using a plasmonic Yagi-Uda nanoantenna array," *Photonics Technol. Lett. IEEE*, vol. 26, no. 22, pp. 2236-2239, 2014.
[20] D. K. Kotter, S. D. Novack, W. D. Slafer, and P. J. Pinhero, "Theory and manufacturing processes of solar nanoantenna electromagnetic collectors," *J. Sol. Energy Eng.*, vol. 132, no. 1, p. 11014, 2010.
[21] Z. Li, H. T. Hattori, and E. G. Mironov, "Charnia-like broadband plasmonic nano-antenna," *J. Mod. Opt.*, vol. 60, no. 10, pp. 790-796, 2013.
[22] CST Microwave Studio, CST GmbH, 2016. http://www.cst.com
[23] P. B. Johnson and R. W. Christy, "Optical constants of the noble metals," *Physical Review B*, vol. 6, Article ID 4370, 1972.
[24] E. Palik, *Handbook of Optical Constants of Solids*. vol. 1, Academic, New York, NY, USA, 1985.

Thi Thanh Kieu Nguyen received the B.S. degree in Computational Physics from Dalat University, Dalat City, Vietnam in 2008, and the M.S. degree in Radio Physics and Electronics – Engineering Physics from the University of Science, Vietnam National University, Ho Chi Minh City in 2015. She is currently Lecturer in Engineering Department, Binh Thuan Province Vocational College, Binh Thuan, Vietnam.

Quang Minh Ngo received the B.S. degree in Information and Communication Technology from Hanoi University of Science and Technology and the MSc. degree in Electronics and Telecommunications from VNU University of Engineering and Technology, Hanoi, Vietnam, in 2000 and 2005, respectively. In 2006, he was awarded the BK21 Doctoral Scholarship to study Electrical Engineering (Photonics) in the Nanophotonics group at the Department of Electrical and Computer Engineering, Ajou University, Suwon, Korea where he received the Ph.D. degree on Feb. 2011. From Sep. 2000 until now, he is a Permanent Researcher of Institute of Materials Science (IMS), Vietnam Academy of Science and Technology (VAST), Hanoi, Vietnam. Since Mar. 2012, he has worked as a Leader of Micro- and Nano-Photonic Research Group at IMS. From Nov. to Dec. 2013, he worked at the Institute of Electronic Fundamental, Paris-Sud University, Orsay, France as a Visiting Professor. From Sep. 2014 to Sep. 2015 and from Feb. 2016 to Feb. 2017, he was a Visiting Scholar of Vietnam Education Foundation at the Department of Physics, Applied Physics and Astronomy, State University of New York at Binghamton, NY, United States and at the Department of Electrical and Electronic Engineering, University of Bristol, Bristol, United Kingdom, respectively. His research interests lie in understanding the theory, simulation and experiment of micro- and nano-photonic structures in the visible and near infrared spectral regions for optical devices, focused on the photonic crystals, plasmonics, and metamaterials. He serves as an active Reviewer for international journals including IEEE/OSA Journal of Lightwave Technology, Journal of Optical Society of America A (and B), Applied Optics, Journal of Applied Physics, Applied Physics Letters.

Truong Khang Nguyen received the B.S. degree in Computational Physics from the University of Science, Vietnam National University, Ho Chi Minh City in 2006, and the M.S. and Ph.D. degrees in Electrical and Computer Engineering from Ajou University in Suwon, Korea in 2013. From Oct. 2013 to Dec. 2014, he worked at Division of Energy Systems Research, Ajou Univerisity, Korea as a postdoctoral fellow. He is currently Head of Division of Computational Physics at Institute for Computational Science, Ton Duc Thang University in Ho Chi Minh City, Vietnam. He has written one chapter book in the area of THz antenna and filed one patent on THz stripline antenna. He serves as a Reviewer for international journals including Journal of Infrared, Millimeter, and Terahertz waves, Journal of Electromagnetic Waves and Applications, Progress in Electromagnetic Research, etc. He was awarded by Central Committee of the Vietnamese Student Association in 2012 and by Vietnamese Embassy in Korea in 2013 for Vietnamese Student in Korea with excellent research achievements. His current research interests include the design and analysis of microwave, millimeter-wave, terahertz wave, and nano-structured antennas.